



Radial T2* mapping reveals early meniscal abnormalities in patients with knee osteoarthritis

Ping-Huei Tsai^{1,2} · Chin-Chean Wong^{3,4} · Wing P. Chan^{5,6} 

Received: 11 August 2021 / Revised: 21 January 2022 / Accepted: 6 February 2022 / Published online: 8 March 2022
© The Author(s), under exclusive licence to European Society of Radiology 2022

Abstract

Objective We aimed to validate a 2D radial T2* mapping method and its ability to reveal subtle alterations in the menisci of patients with knee osteoarthritis (OA).

Methods Of 40 enrolled participants, 20 were diagnosed with OA, and 20 were age- and sex-matched asymptomatic controls. Data from the right knee of each participant were collected using a 1.5-T MRI equipped with a single-channel knee coil. T2* values were acquired using a conventional T2* mapping protocol and a radial T2* mapping method. Mean T2* values in the meniscal white zones, meniscal red zones, and total menisci were calculated. Numerical simulation was performed for validation.

Results Both simulation and clinical data confirmed that 2D radial T2* mapping provided better discrimination than the conventional method. Compared to controls, the OA group showed significantly greater mean (standard deviation) T2* values in the white zones (9.33 [2.29] ms vs. 6.04 [1.05] ms), red zones (9.18 [2.03] ms vs. 6.81 [1.28] ms), and total menisci (9.26 [2.06] ms vs. 6.34 [1.14] ms). Correlations were found between the Lequesne index and the meniscal T2* values in all three regions ($r = 0.528$, $p = 0.017$; $r = 0.635$, $p = 0.003$; and $r = 0.556$, $p = 0.011$, respectively).

Conclusion These findings indicate that in early OA, radial T2* mapping is an alternative means of assessing meniscal degeneration and can be used to monitor its progression.

Key Points

- Radial T2* mapping outperforms Cartesian T2* mapping.
- Radial T2* measurements are useful in assessing meniscal degeneration.
- Meniscal T2* values correlate well with disease severity.

Keywords Knee · Magnetic resonance imaging (MRI) · Meniscus · Osteoarthritis

Abbreviations

MRI	Magnetic resonance imaging
OA	Osteoarthritis
SD	Standard deviation
UTE	Ultra-short echo time

Introduction

Human menisci play important roles in stabilizing and maintaining normal functions in the knee joint. Meniscal damage or degeneration can be related to cartilage volume loss, bone marrow lesions, or altered subchondral bone perfusion after traumatic knee injuries or during the progression of

✉ Wing P. Chan
wingchan@tmu.edu.tw

¹ Department of Medical Imaging and Radiological Sciences, Chung Shan Medical University, Taichung, Taiwan

² Department of Medical Imaging, Chung Shan Medical University Hospital, Taichung, Taiwan

³ Department of Orthopedics, Shuang-Ho Hospital, Taipei Medical University, Taipei, Taiwan

⁴ Department of Orthopedics, School of Medicine, College of Medicine, Taipei Medical University, Taipei, Taiwan

⁵ Department of Radiology, Wan Fang Hospital, Taipei Medical University, No. 111, Xinglong Road, Section 3, Taipei 116, Taiwan

⁶ Department of Radiology, School of Medicine, College of Medicine, Taipei Medical University, Taipei, Taiwan

osteoarthritis (OA) due to altered load distribution and an unstable knee joint [1–4]. The extent of meniscal damage, identified using magnetic resonance imaging (MRI), can be associated with the severity of knee pain [5]. Although the pathological mechanisms of meniscal involvement and the subsequent development of knee OA remain unclear, investigations into the relationship between damage to knee menisci and OA have gained increasing attention, suggestive of the importance of observing the infrastructural changes in menisci during OA progression.

Several quantitative MR measurements, including delayed gadolinium (Gd)-enhanced MRI and mapping of T1 rho and T2, have been developed to reveal the infrastructural information in knee menisci during the various stages of pathological severity or during progression of OA [6–8]. While changes in the concentrations of glycosaminoglycans and proteoglycans in the degenerated menisci can be associated with altered T1 and T1 rho relaxation times, MR T2 measurements are more useful in clinical applications because they do not require injection of contrast agents or advanced sequence programming. T2 values are reportedly reflective of subtle changes in water content and orientation of the collagen fibers in knee menisci; these indicators are signals of meniscal degradation [9, 10], and they correlate with OA severity [11].

Zonal differences in fiber composition, vascularization, nutritional state, and cell metabolism in knee menisci have frequently been emphasized [12–14]. For example, the thick, vascularized outer border of the meniscus is largely composed of circumferential collagen fibers that experience tensile “hoop” stresses with loading, while the tapered, avascular inner edge features higher proteoglycan content [15]. Additionally, the red zone of the meniscus has regenerative potential with good preconditions for improving vascularization and nutritional state. However, the poor healing potential of the inner white zone can lead to increasing risks of early degeneration and failure of meniscus suturing [16], suggestive of the importance of monitoring the early microstructural alterations in the white zone of the meniscus.

Though a useful method for unveiling meniscal heterogeneity and a contributor to clinical diagnosis and treatment, conventional MRI cannot produce adequate signal from the meniscus because the T2 time of the water in this highly collagenous structure is short (approximately 5–8 ms at 1.5 T) and can lead to T2 overestimation. Compared to the Cartesian scheme, radial T2* mapping provides radial sampling and the opportunity to acquire k-space data at the origin directly after excitation without phase encoding, preserving shorter T2 signals. Recent studies have taken advantage of these features, demonstrating the capabilities of 3D ultra-short echo time (UTE) imaging sequencing in revealing the microstructure of the cadaveric meniscus, detecting potential degradation in those at risk of developing OA [17–19]. However, the inhomogeneous slice profile and long acquisition time of a 3D

sequence can restrict its clinical applications. More importantly, William et al indicated that a UTE is not required to study meniscal T2* relaxation, given that only 10% of the pixels in asymptomatic menisci had values smaller than 6.2 ms [18]. A 2D dual-echo radial sequence conjugated with a minimal phase excitation pulse provides an alternative means of detecting meniscal T2* values with more flexibility and less time consumption at a given repetition time [20]. The purpose of this study was to validate a 2D radial T2* mapping method and assess its feasibility for detecting early meniscal abnormalities in patients with OA.

Materials and methods

Simulation

Numerical simulations were performed to investigate the validity of radial T2* mapping, assessing rapid decay signals and the effects of echo time arrangements. Undoubtedly, the noise levels in obtained images will critically affect the accuracy of T2* quantification in clinical applications. With this in mind, we first simulated the T2* relaxation data with short and relatively long T2* times (5 and 8 ms), and then Rician noise was added by applying a series of noise levels (1–10%) according to its amplitude of noise distribution. The data were then fitted using the signals obtained at the corresponding TEs available from either conventional T2* mapping or 2D UTE-based T2* mapping. For each condition, 1000 repetitions were performed to yield 1000 T2* estimates. The accuracy of and variations in the fitted values were evaluated by finding the means and associated standard deviations (SDs) of the T2* values.

Participant enrollment

To validate a 2D radial T2* mapping protocol, 20 asymptomatic people (11 male) were included in this study as approved by the Taipei Medical University-Joint Institutional Review Board in Taipei, Taiwan (Approval No. 201302052), and all participants gave written informed consent. Inclusion criteria were the following: (1) body mass index under 30 kg/m² [21], (2) asymptomatic with a zero Lequesne index [22] in each knee, (3) no MRI-based signals indicating meniscal tears or meniscal intrasubstance fluid, (4) no MRI-based signals indicating abnormal ligaments, and (5) no loss of any portion of the meniscus or a discoid meniscus.

Participation by patients with OA was also approved by the institutional review board, and informed consent was waived due to the retrospective nature of their inclusion (Approval No. N201704004). This group of participants was referred from an orthopedic surgeon who performed routine standardized physical examinations and MR T2* mapping protocols

Table 1 Participant characteristics

	Asymptomatic participants	OA study group
No.	20	20
Age ^a , y	55.9 (9.0)	57.1 (7.9)
Male:female	11:9	11:9
BMI ^a , kg/m ²	23.8 (2.7)	24.8 (2.9)
Lequesne index ^a	0.0 (0.0)	9.7 (1.9)

OA osteoarthritis, BMI body mass index

^a Mean (standard deviation)

from January 2012 through December 2015. Diagnoses were based on American College of Rheumatology Classification Criteria of 1986 as well as the recommendations of the European League Against Rheumatism of 2010 [23–25]. The Kellgren-Lawrence grading system was used to confirm this diagnosis, given its complexity—several radiographic features of OA must be considered, including joint space narrowing and osteophyte development [26]. Inclusion criteria were the following: (1) aged at least 40 years; (2) diagnosis of tibia-femoral OA of the knee by radiography, graded 1 or 2 using the Kellgren-Lawrence scale; and (3) more than one episode of symptomatic knee joint pain rated at least 3 on a 0-to-10 visual analog scale for 10 days.

Exclusion criteria were the following: (1) history of systemic autoimmune rheumatoid disease, (2) septic arthritis, (3) intra-articular fracture involving knee joints, (4) knee arthroscopy, (5) body mass index greater than 30 kg/m², and (6) meniscal tears or intersected articular surfaces shown on MRI [27]. A total of 20 patients with OA (11 male) were included in the study group (Table 1).

Data acquisition

All MR examinations were performed on a 1.5-T clinical MR system (Magnetom Avanto; Siemens Healthineers). The right

knee of each participant was centered in a circularly polarized extremity coil (Siemens Healthcare). Variation in the “magic angle effect” on the meniscus T2* measurement was diminished [28] by aligning the long axis of the leg with the primary magnetic field (B_0). Then, MR-compatible plastic pads were used to immobilize the leg. Pilot images in the three orthogonal planes were obtained by applying several spin-echo sequences: coronal proton density with and without fat saturation, sagittal T2-weighted with fat saturation, and axial proton density with fat saturation.

Subsequently, oblique sagittal T2*-weighted images covering the medial and lateral menisci were acquired using a 2D dual-echo radial imaging sequence, applying six TEs: 1.04, 2.50, 4.00, 6.56, 8.02, and 9.52 ms. All other parameters were kept constant: flip angle, 60°; repetition time, 700 ms; number of slices, 8; slice thickness, 5 mm; slice gap, 20% of slice thickness; projection number, 384; readouts per projection, 256; in-plane resolution, 0.23 mm × 0.23 mm; and acquisition time, 11:30 min. The sequence diagram is shown in Fig. 1. To produce conventional T2* mapping, a multi-slice, multi-echo, gradient-echo sequence was performed, applying the following parameters: TE, 4.38, 11.85, 19.32, 26.79, 33.88, and 40.58 ms; flip angle, 60°; repetition time, 403 ms; matrix size, 256 × 256; in-plane resolution, 0.23 mm × 0.23 mm; slice thickness, 3 mm; slice gap, 20% of slice thickness; number of excitations, 2; number of slices, 17; and acquisition time, 15:30 min. Total acquisition time was less than 40 min.

Data analysis

Selection of regions of interest

The meniscus was anatomically divided into three regions of interest (ROIs) based on vascularization [13]: the white zone (inner 2/3), the red zone (outer 1/3), and the entire meniscus. Two experienced readers (PHT and WPC, experienced 10 years and 22 years, respectively) separately defined the

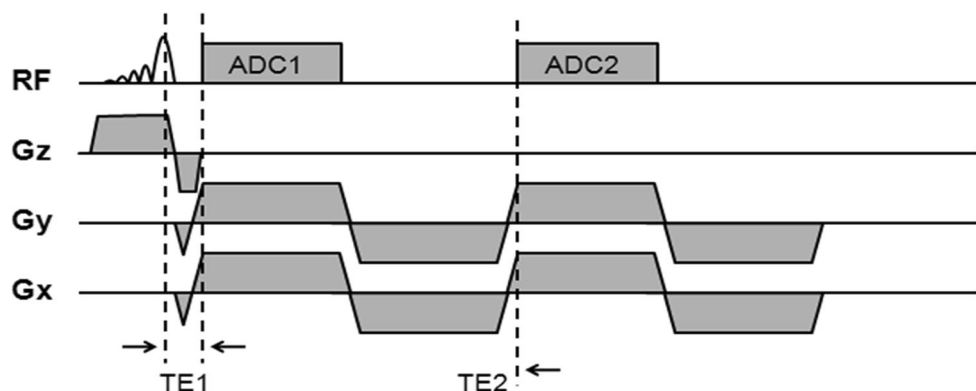
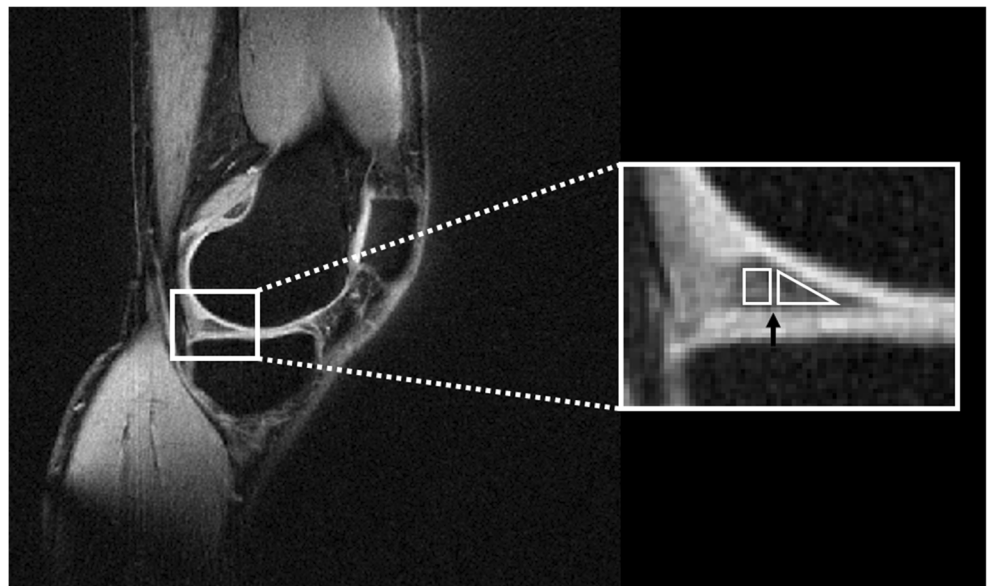


Fig. 1 Schematic sequence diagram of the 2D dual-echo radial sequence. A minimal phase radio frequency pulse used for slice excitation was followed by two simultaneously ramping frequency-encoding gradients along the x and y directions, yielding a radial k -space acquisition at a very

short echo time (first echo). The inverse gradients subsequently performed to rephase the signal were followed by the repeat gradient pairs to obtain the second echo

Fig. 2 Example of placement of the region of interest (ROI) on a sagittal slice of the knee menisci. The ROIs were selected based on an intermediate-echo T2* image (enlarged to the right). The separation between the white zone (inner two-thirds of the meniscus) and the red zone (outer one-third of the meniscus) is indicated by a black arrow



ROIs for three randomly selected participants. Disagreements were resolved by consensus to minimize discrepancies. Intermediate-echo T2* images, which show good contrast between the meniscus and articular cartilage (Fig. 2), were used for ROI selection. Partial volume effects were alleviated by excluding the upper and lower meniscal borders from the ROIs. The signal-to-noise ratios of the acquired meniscal images at various TEs from both protocols were used to make further comparisons.

T2* calculation

Meniscal T2* analyses were conducted on a pixel-by-pixel basis. The T2* values were derived using the least-square single-exponential curve-fitting method on the MATLAB 2019b software platform (Mathworks). Goodness of fit was assessed using R² values, similar to what is used in nonlinear curve fitting [29]. Because the posterior horn of the medial meniscus is the most frequent location of meniscal

degeneration [30, 31], the posterior horns of the medial and lateral menisci were selected as the foci for this study. A mean T2* value was obtained at each pixel by averaging the T2* values at that pixel across every single slice.

Statistical analysis

The Statistical Package for the Social Sciences (SPSS) software, version 20.0, was used to analyze the collected data. Means and SDs of meniscal T2* values from the three ROIs were calculated first. Then, the Dice scores and intra-class correlation coefficients were determined to assess inter-operator and intra-observer differences. Effect sizes and percent differences in the T2* values were derived to compare the discrimination power of the radial T2* mapping scheme with that of the conventional method. Two-way repeated-measures analysis of variance was used to examine differences in T2* values between the three ROIs and to compare the meniscal T2* values between asymptomatic controls and the study

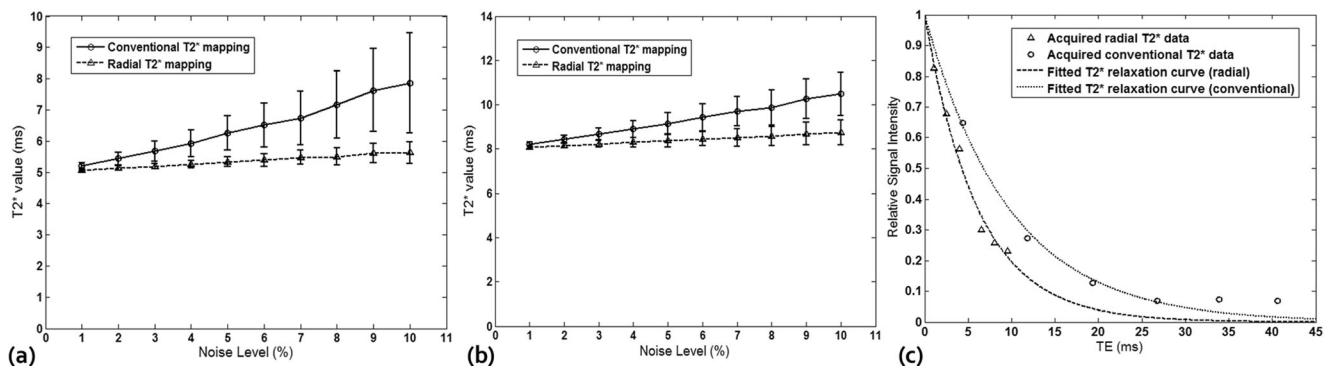
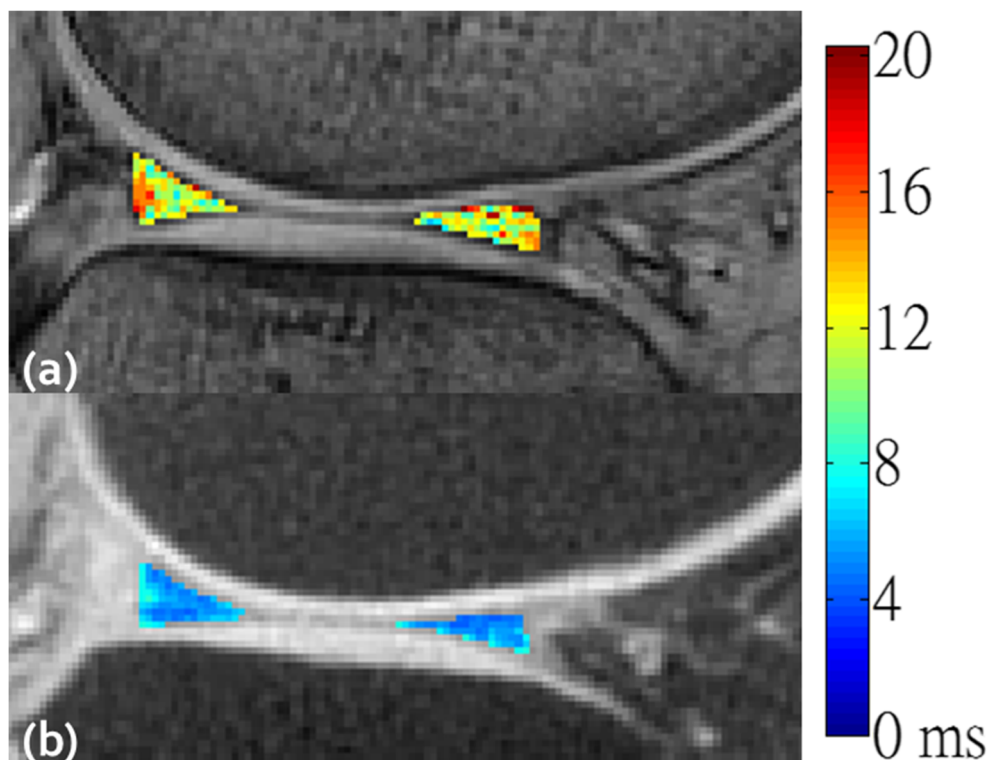


Fig. 3 Comparisons of simulated T2* values, fitted using either Cartesian-based or radial T2* mapping across various noise levels when T2* = 5 ms (a) or T2* = 8 ms (b). The error bars represent the standard

deviations of the derived T2* values from 1000 simulations. The real signal intensities between the two approaches are also shown (c)

Fig. 4 For a sample asymptomatic control, T2* maps derived from conventional T2* mapping (a) and radial T2* mapping (b)



group. The Spearman rank correlation was used to analyze associations between T2* values and Lequesne indices in the study group. Corrections for multiple testing were applied using the Benjamini-Hochberg method for the false discovery rate [32]. Statistical significance was recognized when the corrected p value was < 0.05 .

Results

Simulation data

Simulated T2* fittings, applying two T2* times (5 ms and 8 ms) across a range of noise levels and applying two T2* mapping approaches, are compared in Fig. 3. In conventional T2* mapping, the derived T2* values increased from 5 to 7.86 ms (57.2% error) and from 8 to 10.49 ms (31.1% error), showing enlargement with increasing noise, particularly at the shortest

T2* relaxation time, when arrangement of the echo times is inappropriate. In contrast, the fitted T2* values were more accurate and less sensitive to noise using radial T2* mapping, no matter the T2* time; more signals were obtained even in the late echo image. In vivo human meniscal T2* maps derived using the two approaches are shown in Fig. 4. Overestimations of the meniscal T2* values are shown in the Cartesian-based T2* map. The signal-to-noise ratios of the acquired images at the six TEs are greater using the radial T2* approach (46.5/38.1/31.6/16.8/14.4/13.0) than the conventional T2* approach (27.9/11.8/5.5/2.9/3.1/3.0).

Comparisons of effect sizes and percentage differences across the two methods

Table 1 shows participant characteristics of the study group and the age- and sex-matched controls (mean [SD] age, 57.1 [7.9] years and 55.9 [9.0] years, respectively). The radial T2*

Table 2 Effect sizes of the T2* values for the combined group of asymptomatic controls and patients with osteoarthritis (OA)

	Conventional T2* mapping	Radial T2* mapping
White zone	0.174	0.460 [▲]
Red zone	0.247	0.327 [▲]
Total meniscus	0.214	0.433 [▲]

[▲] Higher effect size between asymptomatic participants and OA patients

Table 3 Percent increase in T2* values in patients with early osteoarthritis compared to asymptomatic controls

	Conventional T2* mapping	Radial T2* mapping
White zone	25%	54%
Red zone	24%	35%
Total meniscus	24%	46%

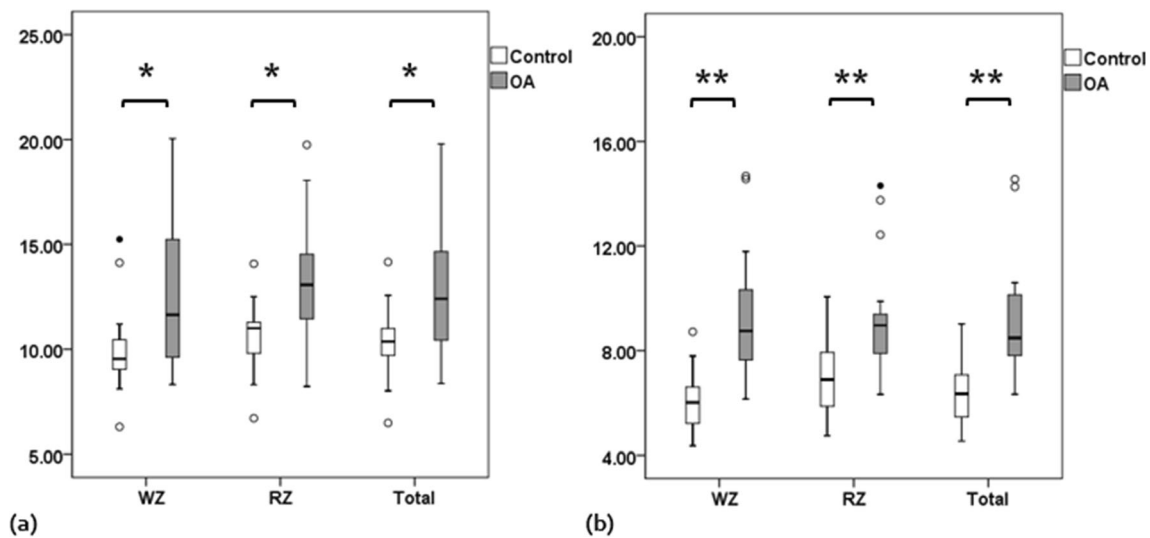


Fig. 5 Statistical comparisons of the mean T2* values in the white zones (WZ), red zones (RZ), and total menisci (Total) between patients with early osteoarthritis (OA) and asymptomatic controls using conventional

T2* mapping (a) and radial T2* mapping (b). Significant differences after correcting for multiple comparisons are indicated (* $p < 0.05$; ** $p < 0.001$)

mapping showed a larger effect size than conventional T2* mapping in all three ROIs (Table 2). Additionally, using conventional T2* mapping, meniscal T2* values in the study group were 24 to 25% greater than those in the controls in all three ROIs. In contrast, using radial T2* mapping, the increase is more than 35% in all three ROIs—up to 54% in the white zone (Table 3).

correlation coefficients for the ROIs were greater than 0.85 and 0.91, respectively, indicating good reproducibility.

Comparisons of T2* values between groups using two mapping methods

Correlations between T2* values and the Lequesne index in the OA group

Mean (SD) meniscal T2* values were compared between groups and mapping methods. Using conventional T2* mapping, the T2* values in the white zones, red zones, and total menisci were 9.92 (1.92), 10.66 (1.48), and 10.28 (1.51) ms, respectively, in the control group. These were significantly greater for the patients with OA: 12.43 (3.35), 13.19 (2.75), and 12.72 (2.93) ms, respectively ($p < 0.05$). See Fig. 5(a). On the other hand, using radial T2* mapping, the values were 6.04 (1.05), 6.81 (1.28), and 6.34 (1.14) ms, respectively, for the control group and 9.33 (2.29), 9.18 (2.03), and 9.26 (2.06) ms, respectively, for the study group ($p < 0.001$). See Fig. 5(b). The three ROIs did not differ significantly within either mapping method. The derived Dice scores and intra-class

Table 4 shows the relationship between the T2* values and the Lequesne index in the study group. Although T2* values from conventional mapping in the white zones, red zones, and total menisci did not significantly correlate with the Lequesne index ($r = 0.306, p = 0.189$; $r = 0.252, p = 0.284$; and $r = 0.278, p = 0.235$, respectively), moderate correlations were found when the T2* values were derived using radial T2* mapping ($r = 0.528, p = 0.017$; $r = 0.635, p = 0.003$; and $r = 0.556, p = 0.011$, respectively).

Table 4 Correlation between T2* values and the Lequesne index in patients with early osteoarthritis

	Conventional T2* mapping	Radial T2* mapping
White zone	0.306 ($p = 0.189$)	0.528 ($p = 0.017$)
Red zone	0.252 ($p = 0.284$)	0.635 ($p = 0.003$)
Total meniscus	0.278 ($p = 0.235$)	0.556 ($p = 0.011$)

Discussion

Our simulated data and preliminary results indicate that 2D T2* mapping in in vivo human menisci using non-Cartesian radial sampling is both feasible and reliable. These simulations show that estimates of meniscal T2* values are reasonably robust to discrepant noise levels. Although the Cartesian-based T2* mapping method is more available with commercial MR scanners, the derived T2* values for human menisci were significantly overestimated, particularly in the white zone, consisting of less vasculature and greater proteoglycan content compared to the peripheral red zone. These differences result in relatively faster T2 relaxation [33], possibly leading to poorer sensitivity to subtle matrix changes in the menisci, thus restricting its clinical application. In contrast, using 2D radial T2* mapping, the derived T2* values are less

prone to inaccuracy, suggesting its superiority in detecting early meniscal abnormalities *in vivo*.

The ability of UTE-based T2* mapping to unveil the rapid decay signal as well as pathological changes in the menisci has been recently reported [18, 34–37]. Meniscal calcifications were morphologically and quantitatively evaluated using the UTE technique [35]. Williams et al examined the diagnostic potential of UTE-T2* mapping to detect meniscal degeneration and found elevated T2* values in participants with developing OA [18]. Meniscal matrix changes after anterior cruciate ligament injury can be shown using UTE-based T2* mapping [36]. Our findings agree: mean meniscal T2* values tended to be greater in patients with mild OA compared with age- and sex-matched controls. We also found moderate correlations between mean meniscal T2* values and the Lequesne index in the OA group, confirming a potential diagnostic value of the 2D radial T2* mapping method. The human knee meniscus is not a homogeneous tissue; the orientation and type of collagen fibers and the blood supply to the meniscus vary substantially between varietal zones [38, 39]. Zonal differences in meniscal T2 values have been examined in healthy and asymptomatic people, reflecting the discrepant meniscal matrix and varying degree of vascularity [10, 40]. Additional variability can be seen in normal canine menisci when MRI UTE T2* is applied [41], implying that richer information can be provided by zonal analysis on a 2D radial T2* map. We found that T2* values tended to increase in asymptomatic controls from the inner white zone to the outer red zone. Moreover, one of the most common degenerative tears (the horizontal-cleavage tear) usually begins near the inner meniscus and extends out toward the periphery during natural meniscal degradation [42]. The difference in white zone T2* values between those with early OA and controls was up to 54%, demonstrating that 2D radial T2* mapping has the potential to assess early degeneration in white zone menisci.

This study has a few limitations. First, small groups were used for both the study population and asymptomatic controls, possibly leading to selection bias in the meniscal T2* values and related zonal differences in menisci. Using G*Power software, more than 134 participants should be recruited, given our effect size ($\rho = 0.3$, $\alpha = 0.05$, and $1 - \beta = 0.95$). Second, the total acquisition time of 2D dual-echo UTE imaging is longer than that of conventional T2* mapping when acquiring the same number of slices. Taking advantage of parallel imaging techniques should provide further benefits. Third, the partial volume effect can be different in the two T2* protocols because of the variable slice thickness resulting from the discrepant RF excitation pulses. Finally, a single-component exponential T2* fitting was performed in this study. Although this method has been frequently used to generate meniscal T2* maps, bi-component T2* fitting can provide more extensive information of human menisci [43].

In conclusion, 2D radial T2* mapping is superior in detecting early meniscal degeneration compared with conventional T2* mapping, evidenced by clinical assessments. These findings show that this technique provides an alternative means of revealing infrastructural changes in knee menisci in early OA, and it has diagnostic potential in clinical applications.

Funding This study was funded by grant Investigator Initiated Trials no. IIT-1072-1 at Taipei Medical University and grant no. NSC 103-2221-E-038-015- and NSC 102-2221-E-038-001- at the Ministry of Science and Technology, Taiwan.

Declarations

Guarantor The scientific guarantor of this publication is Professor Wing P. Chan.

Conflict of interest The authors of this manuscript declare no relationships with any companies whose products or services may be related to the subject matter of the article.

Statistics and biometry No complex statistical methods were necessary for this paper.

Informed consent All asymptomatic participants signed written informed consent.

Ethical approval Institutional Review Board approval was obtained.

Methodology

- Prospective
- Observational
- Performed at one institution

References

1. Antony B, Driban JB, Price LL et al (2017) The relationship between meniscal pathology and osteoarthritis depends on the type of meniscal damage visible on magnetic resonance images: data from the Osteoarthritis Initiative. *Osteoarthritis Cartilage* 25:76–84
2. Englund M, Guermazi A, Roemer FW et al (2010) Meniscal pathology on MRI increases the risk for both incident and enlarging subchondral bone marrow lesions of the knee: the MOST Study. *Ann Rheum Dis* 69:1796–1802
3. Tsai PH, Lee HS, Siow TY et al (2016) Abnormal perfusion in patellofemoral subchondral bone marrow in the rat anterior cruciate ligament transection model of post-traumatic osteoarthritis: a dynamic contrast-enhanced magnetic resonance imaging study. *Osteoarthritis Cartilage* 24:129–133
4. Tsai PH, Wong CC, Chan WP, Lu TW (2019) The value of MR T2* measurements in normal and osteoarthritic knee cartilage: effects of age, sex, and location. *Eur Radiol* 29:4514–4522
5. MacFarlane LA, Yang H, Collins JE et al (2017) Associations among meniscal damage, meniscal symptoms and knee pain severity. *Osteoarthritis Cartilage* 25:850–857
6. Sigurdsson U, Müller G, Siversson C et al (2016) Delayed gadolinium-enhanced MRI of meniscus (dGEMRIM) and cartilage

- (dGEMRIC) in healthy knees and in knees with different stages of meniscus pathology. *BMC Musculoskelet Disord*. <https://doi.org/10.1186/s12891-12016-11244-z>
7. Rauscher I, Stahl R, Cheng J et al (2008) Meniscal measurements of T1rho and T2 at MR imaging in healthy subjects and patients with osteoarthritis. *Radiology* 249:591–600
 8. Hagiwara S, Takao S, Yu H et al (2017) Zonal differences of T1rho and T2 relaxation times of advanced osteoarthritis knees meniscus. *Osteoarthritis Cartilage* 25:S258–S259
 9. Eijgenraam SM, Bovendeert FAT, Verschuieren J et al (2019) T2 mapping of the meniscus is a biomarker for early osteoarthritis. *Eur Radiol* 29:5664–5672
 10. Chiang SW, Tsai PH, Chang YC et al (2013) T2 values of posterior horns of knee menisci in asymptomatic subjects. *PLoS One* 8: e59769
 11. Hada S, Ishijima M, Kaneko H et al (2017) The degeneration of medial meniscus detected by T2 mapping MRI according to the severity of medial knee osteoarthritis. *Osteoarthritis Cartilage* 25: S250–S251
 12. Fuller ES, Smith MM, Little CB, Melrose J (2012) Zonal differences in meniscus matrix turnover and cytokine response. *Osteoarthritis Cartilage* 20:49–59
 13. Day B, Mackenzie WG, Shim SS, Leung G (1985) The vascular and nerve supply of the human meniscus. *Arthroscopy* 1:58–62
 14. Tarafder S, Park G, Lee CH (2020) Explant models for meniscus metabolism, injury, repair, and healing. *Connect Tissue Res* 61: 292–303
 15. Ghosh P, Taylor TK (1987) The knee joint meniscus. A fibrocartilage of some distinction. *Clin Orthop Relat Res* 224:52–63
 16. Weber J, Koch M, Angele P, Zellner J (2018) The role of meniscal repair for prevention of early onset of osteoarthritis. *J Exp Orthop* 5:10
 17. Omoumi P, Bydder G, Znamirovski RM, Du J, Statum SS, Chung CB (2010) Infrastructure of menisci with MR imaging. Proceedings of the 18th meeting of ISMRM
 18. Williams A, Qian Y, Golla S, Chu CR (2012) UTE-T2* mapping detects sub-clinical meniscus injury after anterior cruciate ligament tear. *Osteoarthritis Cartilage* 20:486–494
 19. Yi J, Lee YH, Song HT, Suh JS (2018) Comparison of T2* mapping between regular echo time and ultrashort echo time with 3D cones at 3 tesla for knee meniscus. *Medicine (Baltimore)* 97:e13443
 20. Tsai PH, Huang TY, Chung HW, Tsai FY, Chan WP (2013) Quantitative T2* mapping of in vivo human meniscus using 2D dual echo radial sequence with minimal phase excitation pulse at 3 T. In: Proceedings of the 21st Meeting of ISMRM, p 3513
 21. Grotle M, Hagen KB, Natvig B, Dahl FA, Kvien TK (2008) Obesity and osteoarthritis in knee, hip and/or hand: an epidemiological study in the general population with 10 years follow-up. *BMC Musculoskelet Disord*. <https://doi.org/10.1186/1471-2474-1189-1132>
 22. Dawson J, Linsell L, Doll H et al (2005) Assessment of the Lequesne index of severity for osteoarthritis of the hip in an elderly population. *Osteoarthritis Cartilage* 13:854–860
 23. Altman R, Asch E, Bloch D et al (1986) Development of criteria for the classification and reporting of osteoarthritis. Classification of osteoarthritis of the knee. Diagnostic and Therapeutic Criteria Committee of the American Rheumatism Association. *Arthritis Rheum* 29
 24. Zhang W, Doherty M, Peat G et al (2010) EULAR evidence-based recommendations for the diagnosis of knee osteoarthritis. *Ann Rheum Dis* 69:483–489
 25. Hochberg MC, Altman RD, April KT et al (2012) American College of Rheumatology 2012 recommendations for the use of non-pharmacologic and pharmacologic therapies in osteoarthritis of the hand, hip, and knee. *Arthritis Care Res* 64:465–474
 26. Kellgren JH, JS L (1957) Radiological assessment of osteoarthrosis. *Ann Rheum Dis* 16:494–502
 27. Howell R, Kumar NS, Patel N, Tom J (2014) Degenerative meniscus: pathogenesis, diagnosis, and treatment options. *World J Orthop* 5:597–602
 28. Bydder M, Rahal A, Fullerton GD, Byder GM (2007) The magic angle effect: a source of artifact, determinant of image contrast, and technique for imaging. *J Magn Reson Imaging* 25:290–300
 29. Bates D, Watts D (1988) Nonlinear regression: iterative estimation and linear approximations. In: *Nonlinear regression analysis and its applications*, xxx edn. Wiley, Location, pp 33–66
 30. Fukuta S, Masaki K, Korai F (2002) Prevalence of abnormal findings in magnetic resonance images of asymptomatic knees. *J Orthop Sci* 7:287–291
 31. Argin M, Dastan AE, Kaya Bicer E, Kaya H, Taskiran E (2020) Stress radiography findings in medial meniscus posterior root tears. *Knee* 27:1542–1550
 32. Storey JD (2002) A direct approach to false discovery rates. *J R Statist Soc B* 64:479–498
 33. Michalek AJ, Kuxhaus L, Jaremczuk D, Zaino NL (2018) Proteoglycans contribute locally to swelling, but globally to compressive mechanics, in intact cervine medial meniscus. *J Biomech* 74:86–91
 34. Bae WC, Tadros AS, Finkenstaedt T, Du J, Statum S, Chung CB (2021) Quantitative magnetic resonance imaging of meniscal pathology ex vivo. *Skeletal Radiol*. <https://doi.org/10.1007/s00256-00021-03808-00256>
 35. Omoumi P, Bae WC, Du J et al (2012) Meniscal calcifications: morphologic and quantitative evaluation by using 2D inversion-recovery ultrashort echo time and 3D ultrashort echo time 3.0-T MR imaging techniques—feasibility study. *Radiology* 264:260–268
 36. Chu CR, Williams AA, West RV et al (2014) Quantitative magnetic resonance imaging UTE-T2* mapping of cartilage and meniscus healing after anatomic anterior cruciate ligament reconstruction. *Am J Sports Med* 42:1847–1856
 37. Xue YP, Jang H, Byra M et al (2021) Automated cartilage segmentation and quantification using 3D ultrashort echo time (UTE) cones MR imaging with deep convolutional neural networks. *Eur Radiol*. <https://doi.org/10.1007/s00330-00021-07853-00336>
 38. Aspden RM, Yarker YE, Hukins DWL (1985) Collagen orientations in the meniscus of the knee joint. *J Anat* 140:371–380
 39. Abbadessa A, Crecente-Campo J, Alonso MJ (2021) Engineering anisotropic meniscus: zonal functionality and spatiotemporal drug delivery. *Tissue Eng Part B Rev* 27:133–154
 40. Tsai PH, Chou MC, Lee HS et al (2009) MR T2 values of the knee menisci in the healthy young population: zonal and sex differences. *Osteoarthritis Cartilage* 17:988–994
 41. Pownder SL, Hayashi K, Caserto BG et al (2018) Quantitative magnetic resonance imaging and histological comparison of normal canine menisci. *Vet Comp Orthop Traumatol* 31:452–457
 42. Setton LA, Guilak F, Hsu EW, Vail TP (1999) Biomechanical factors in tissue engineered meniscal repair. *Clin Orthop Relat Res* 367:S254–S272
 43. Juras V, Apprich S, Zbyň Š et al (2014) Quantitative MRI analysis of menisci using bi-exponential T2* fitting with a variable echo time sequence. *Magn Reson Med* 71:1015–1023

Publisher's note Springer Nature remains neutral with regard to jurisdictional claims in published maps and institutional affiliations.